AIP | Applied Physics Letters

Characterization and manipulation of the "saturation" effect by changing the surface temperature of a dielectric barrier discharge actuator

Ryan Durscher, Scott Stanfield, and Subrata Roy

Citation: Appl. Phys. Lett. **101**, 252902 (2012); doi: 10.1063/1.4772004
View online: http://dx.doi.org/10.1063/1.4772004
View Table of Contents: http://apl.aip.org/resource/1/APPLAB/v101/i25
Published by the American Institute of Physics.

Related Articles

Particle-in-cell simulations of the runaway breakdown of nitrogen
J. Appl. Phys. 112, 113302 (2012)

Femtosecond laser guiding of a high-voltage discharge and the restoration of dielectric strength in air and nitrogen
Phys. Plasmas 19, 123502 (2012)

Compact high-speed reciprocating probe system for measurements in a Hall thruster discharge and plume
Rev. Sci. Instrum. 83, 123503 (2012)

On the streamer propagation in methane plasma discharges
J. Appl. Phys. 112, 113301 (2012)

One-dimensional hybrid-direct kinetic simulation of the discharge plasma in a Hall thruster
Phys. Plasmas 19, 113508 (2012)

Additional information on Appl. Phys. Lett.

Journal Homepage: http://apl.aip.org/
Journal Information: http://apl.aip.org/about/about_the_journal
Top downloads: http://apl.aip.org/features/most_downloaded
Information for Authors: http://apl.aip.org/authors

ADVERTISEMENT

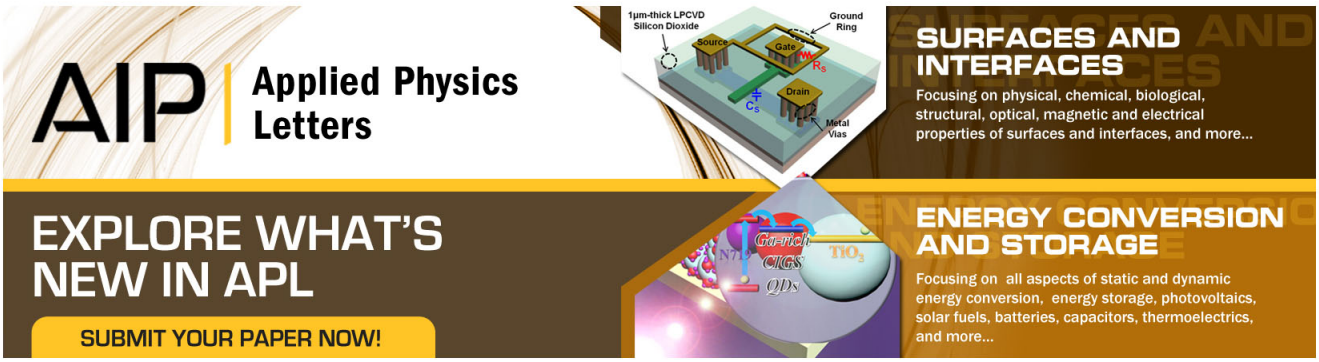

Characterization and manipulation of the "saturation" effect by changing the surface temperature of a dielectric barrier discharge actuator

Ryan Durscher,[1] Scott Stanfield,[2] and Subrata Roy[1,a)]
[1]*Applied Physics Research Group, Department of Mechanical & Aerospace Engineering, University of Florida, Gainesville, Florida 32611, USA*
[2]*Spectral Energies, LLC, Dayton, Ohio 45431, USA*

(Received 23 October 2012; accepted 28 November 2012; published online 17 December 2012)

The thrust produced by a sinusoidally driven dielectric barrier discharge actuator in quiescent air is known to increase with a power law of the applied voltage. For voltages greater than a threshold, the exponent of the power law reduces limiting the thrust increase and the actuator is said to have "saturated," limiting the actuator's usefulness. The onset of saturation is visually correlated by the inception of filamentary discharge events. In this letter, the flow transition to the saturation condition is characterized. Furthermore, the saturation effect can be manipulated by changing the local surface temperature of the dielectric. © *2012 American Institute of Physics*. [http://dx.doi.org/10.1063/1.4772004]

In general, the dielectric barrier discharge (DBD) consists of one exposed and one horizontally displaced encapsulated electrodes separated by a dielectric medium. The presence of the dielectric medium limits the average current density due to an accrual of charge on the surface.[1] This allows the device to operate at moderate pressures without transitioning to an arc discharge, as well as, creates a self-limiting effect which extinguishes the discharge by locally reducing the alternating electric field.[1] This non-thermal discharge has found numerous industrial applications including, but not limited to, ozone generation, biomedical sterilization, surface modification, pollution control, and more recently fluidic actuation.[1,2] It is this latter use that is of particular interest in this letter.

The DBD actuator, as shown in Fig. 1, generates a surface discharge with modest power requirements, on the order of 10-100's of watts per unit length of the actuator. As the discharge expands along the dielectric surface, momentum is transferred to the surrounding fluid, generating a near surface "wall jet." Various parametric studies have focused on increasing the velocity and momentum transfer of this wall jet.[2–4] A metric often used to quantify the wall jet is thrust, which has been interpreted as a measure of the reaction force on the dielectric plate as a result of the plasma induced body force and fluidic shearing effects. In an optimization study by Thomas *et al.*,[5] it was shown that the dielectric thickness, dielectric constant, and driving frequency had a strong effect on the amount of thrust generated. In this investigation, the dielectric thickness, dielectric constant, and driving frequency ranged from 0.15 to 6.35 mm, 2.0 to 6.0, and 1 to 8 kHz, respectively. Moreover, the thrust produced, T, was shown to increase as a power law ($T \propto V^{3.5}$) with increasing voltage, V, up to a threshold voltage. Beyond this threshold voltage, the thrust no longer increased as sharply and the DBD actuator was said to have "saturated," limiting the use of the device. The onset of this saturation effect was associated with a sharp increase in power consumption, and visually correlated with the initiation of filamentary discharge events. The appearance of a DBD actuator is typically described as many glow-like events distributed along the span of the electrode. Thomas *et al.*[5] found that the use of thicker dielectrics with lower dielectric constants and lower driving frequencies delayed the saturating transition, allowing higher voltages to be applied. This in turn maximized the thrust production of the DBD actuator, which from an applications standpoint, might improve the fluidic control authority of the device.

In this letter, the velocity field induced by the DBD actuator in quiescent, atmospheric pressure air is characterized using particle image velocimetry (PIV) for conditions prior to and during saturation. Furthermore, with the use of infrared thermography, it is shown that the surface temperature of the dielectric barrier plays a crucial role in the transition of the glow discharge events to filamentary discharge events. Based on these results, it is shown that the saturation effect can be manipulated by changing the local surface temperature of the dielectric.

A schematic of the DBD actuator configuration used in this study is shown in Fig. 1. The exposed and encapsulated electrodes were made of 10 cm long and 70 μm thick copper, with widths of 10 and 50 mm, respectively. The dielectric material used was 3 mm thick borosilicate glass. The

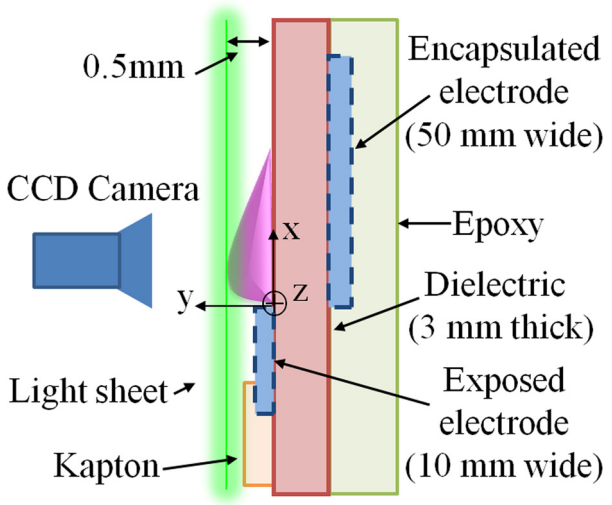

FIG. 1. Cross-sectional schematic shows details of the DBD actuator geometry along with the orientation of the PIV system (not to scale).

a)Electronic mail: roy@ufl.edu. URL: http://aprg.mae.ufl.edu/roy/.

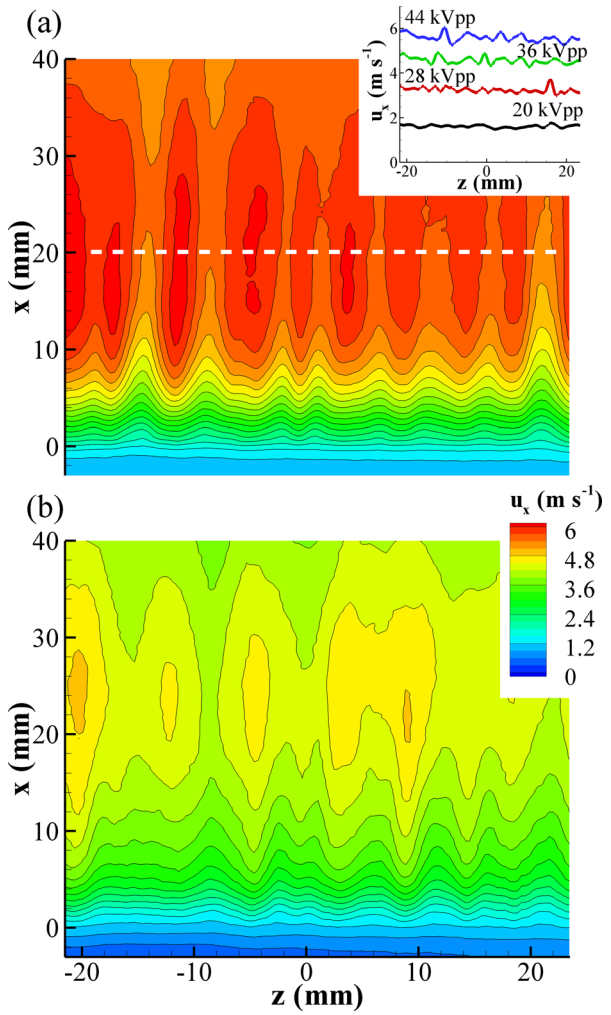

FIG. 2. Time averaged velocity field (a) prior to and (b) during saturation for an approximately constant applied voltage of 44 kVpp at 2 kHz. The inlaid image in (a) depicts the spanwise variations in the primary velocity component, u_x, along $x = 20$ mm (denoted by dashed line) for various voltages.

encapsulated electrode was encased within epoxy to prevent breakdown on the lower surface of the actuator. Similarly, 84 μm thick Kapton tape was placed overtop the back edge of the exposed electrode to prevent breakdown. The discharge was generated by powering both electrodes with sinusoidal voltages of equal magnitude, but opposing polarity imposed using a 180° phase shift. The dissipated power was calculated from the averaged product of the voltage and current waveforms measured for each electrode.

The velocity flow field was measured using a particle image velocimetry system consisting of a Nd:YAG, dual cavity pulsed 532 nm laser, and a CCD camera with a pixel resolution of 2048 × 2048 square pixels. The laser light sheet was positioned parallel to the surface of the DBD, as shown in Fig. 1, and illuminated vaporized Ondina oil. In general, >400 image pairs were captured during each run at a sampling rate of 7.2 Hz. These image pairs were subjected to a cross-correlation multi-grid procedure. Outliers were detected and removed using a recursive, spatial outlier detection scheme.[6] Additional details about the PIV system used can be found in Durscher and Roy.[7]

An infrared camera with a spectral range of 7.5–13 μm and a pixel resolution of 320 × 240 square pixels was aligned at a relative angle of 11° ± 0.2° to the surface, and was used to determine the surface temperature of the dielectric during operation of the DBD actuator. The working distance between the DBD actuator and infrared camera, the ambient temperature and humidity, and the emissivity of the borosilicate glass were measured as 0.3 ± 0.005 m, 20 ± 2 °C, 66 ± 3% RH, and 0.89 ± 0.03, respectively. These quantities were considered for the surface temperature measurements.

It was observed that at particular voltages, the glow-to-filamentary transition was very rapid, and was treated as instantaneous; the breakdown process, however, was delayed by approximately 10-100's of seconds at potentials slightly below this threshold voltage. As shown in Fig. 2, this delayed transition process allowed for a direct comparison between the measured velocity fields prior to (Fig. 2(a)), and immediately after transition of the discharge (Fig. 2(b)) for an approximately constant applied voltage of 44 kVpp at 2 kHz. In Fig. 2, the time averaged velocity field substantially decreased as the discharge events transitioned from a glow-like state to a filamentary one. We also note that although the force from a DBD actuator is generally considered to be uniform along the electrode span, the time averaged induced velocity field does have significant spanwise variations in the primary velocity component, u_x (see inlaid image in Fig. 2(a)). Standard deviations along discrete spanwise cuts were found to be as high as 0.5 m s^{-1} (or ~10% of the maximum velocity) at the higher frequencies investigated (5 and 7 kHz).

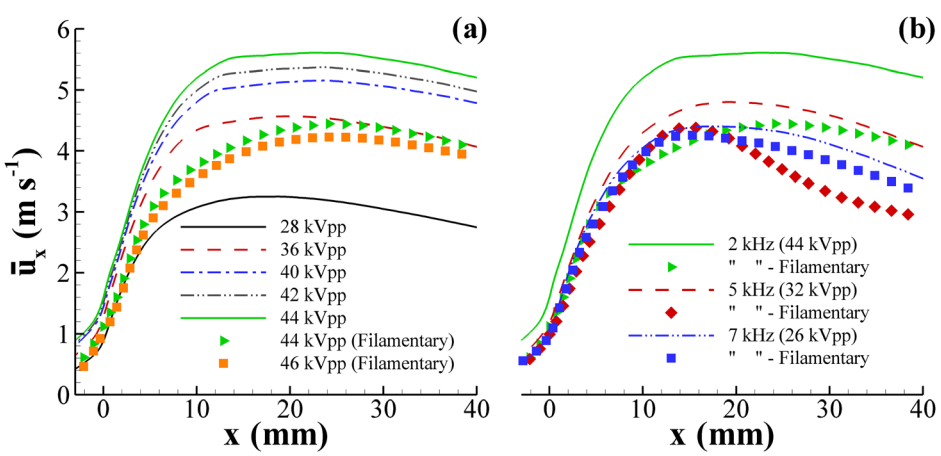

FIG. 3. Spanwise average of the streamwise velocity, $\bar{u}_x$, as a function of streamwise position for various (a) voltages at 2 kHz and (b) frequencies. Conditions corresponding to the presence of filamentary features are denoted by solid symbols.

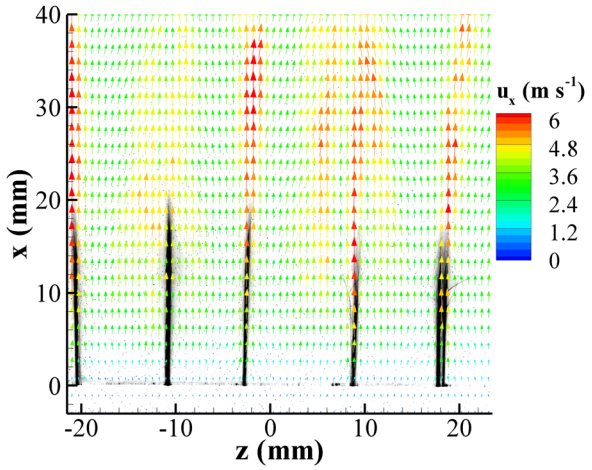

FIG. 4. Instantaneous vector field overlaying an image of the discharge during saturation for an applied voltage of 44 kVpp at 2 kHz.

The decrease in the averaged velocity field during the filamentary mode is more clearly seen in Fig. 3(a), which depicts the spanwise average of the streamwise velocity, $\bar{u}_x$, as a function of streamwise position for various voltages at 2 kHz. As expected, an increase in velocity was associated with an increase in voltage prior to saturation; once the discharge transitioned to a filamentary mode at approximately 44 kVpp for 2 kHz, however, a substantial decrease in velocity was measured. At higher voltages, on the order of 46 kVpp, the transition process was seemingly instantaneous, and again a decrease in velocity was measured. These trends were independent of frequency, as shown in Fig. 3(b).

The saturation effect of the actuator has been previously associated with a decrease in measured thrust.[5] Given that thrust is a measure of the transferred momentum, a quantity integrated over the entire discharge volume, a reduction in the average induced velocity over the discharge volume is expected. However, that does not mean that the velocity field after saturation cannot locally have peak values. As shown in Fig. 4, the instantaneous velocities measured near the filaments were found to be comparable to that of velocities prior to saturation.

As previously stated, for a given frequency, it was found possible to delay the glow-to-filamentary transition process by carefully choosing the applied voltage. In some experiments, this transition process was found to be delayed by 100's of seconds. Such a drastic relative difference between the transition delay and the applied frequency, led to the belief that dielectric heating, which operates on a substantial slower time scale, may be playing a role in the transition process. To investigate its effect, the surface temperature of the actuator and the visible light emission of the plasma were recorded simultaneously. In general, it was found that the filamentary features did not become prominent until the surface temperature of the borosilicate glass was approximately greater than 50 °C (Figs. 5(a)–5(c)). Furthermore, it was found that a glow-to-filamentary transition could be selectively realized without affecting other regions of the discharge by locally heating the dielectric. To accomplish this, the borosilicate glass was locally heated using a hot air gun to a temperature of approximately 90 °C. As shown in Fig. 5(d), where the right side of the actuator was locally pre-heated, the filamentary features immediately occurred when the discharge was established. Moreover, the filamentary features are initially concentrated on the right side of the actuator. Over time, the filaments did begin to encompass the entire span of the exposed electrode (Figs. 5(e) and 5(f)). These results were repeated so that the left side of the actuator was pre-heated as opposed to the right, as shown in Figs. 5(g)–5(i). In both cases, the preheated or filamentary side extended in the streamwise direction well past the unheated glow-like side. The presence of the filaments increased the net power consumption of the device by 30%–40% for the same applied voltage (Table I).

The temperature differences between electrons, vibrational states, and neutral species in the nonequilbrium discharge of the DBD is maintained by a balance between excitation and relaxation processes. This balance may be disrupted however, resulting in a contraction, or "self-compression,"[8] of the plasma, which is consistent with the filamentary discharge events observed at saturation. Within this contraction, the

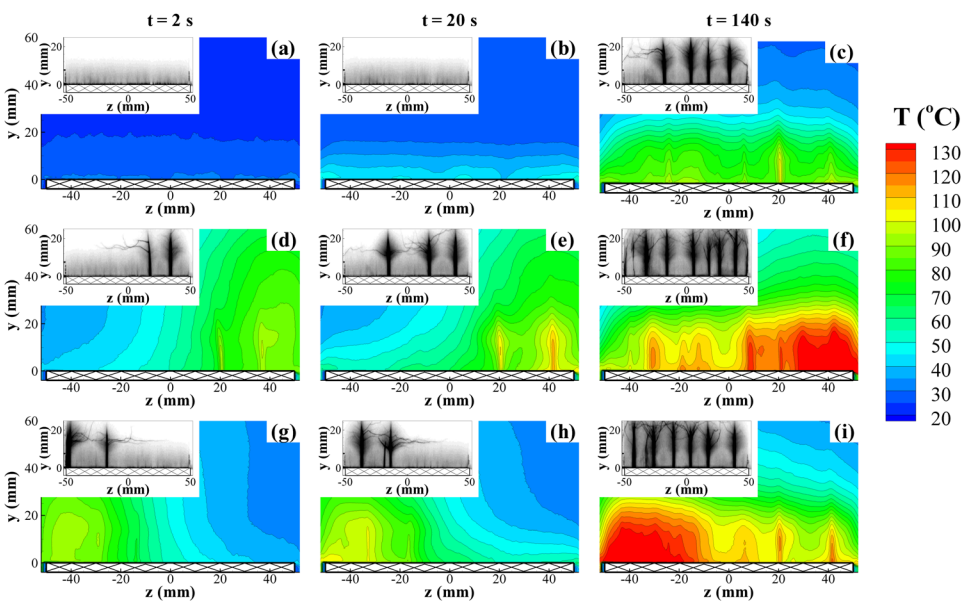

FIG. 5. The temperature distribution along the surface of a DBD actuator operated at 44 kVpp and 2 kHz with increasing (from left to right) time. For images ((a)–(c)) no initial heat addition was provided, while for ((d)–(f)) the right half and for ((g)–(i)) the left half were initially heated to ~90 °C. The corresponding visual appearance of the discharge is provided in the inset images.

TABLE I. Power consumption for a constant voltage (44 kVpp) and frequency (2 kHz) prior to and during the filamentary discharge transformation.

	Power (W)	$\left\lvert \frac{P_{Filamentary}}{P_{Non-filamentary}} - 1 \right\rvert$ (%)
No heat addition (non-filamentary)	23.5 ± 0.8	…
No heat addition (filamentary)	33.2 ± 2.4	41 ± 11
Right half heated (filamentary)	32.2 ± 1.9	37 ± 9
Left half heated (filamentary)	30.7 ± 1.7	31 ± 8

nonequilibrium system attempts to restore itself to a quasi-equilibrium state.[8] As described by Staack *et al.*,[9] the glow-to-filamentary transition of an initially stable DC glow discharge in a monoatomic gas can be described by the ionization overheating instability (IOI), which is given by the positive feedback loop

$$\uparrow \delta T \Rightarrow \downarrow \delta n \Rightarrow \uparrow \delta(E/n) \Rightarrow \uparrow \delta T_e \Rightarrow \uparrow \delta k_i \Rightarrow \uparrow \delta n_e \Rightarrow \uparrow \delta T. \tag{1}$$

In Eq. (1), δ is the differential operator, T is the neutral gas temperature, n is the number density of the neutral species, E/n is the reduced electric field, T_e is the electron temperature, k_i is the ionization rate constant, and n_e is the electron number density. For a molecular gas, as is the case of a DBD actuator operated in air, intermediate vibrational modes (T_{Vib}) must be considered since an increase in electron concentration does not lead directly to gas heating ($\uparrow \delta n_e \Rightarrow \uparrow \delta T_{Vib} \Rightarrow \uparrow \delta T$), though the rest of the processes described in Eq. (1) remain the same. From Eq. (1), a differential increase in the aforementioned parameters (or decrease in the number density of the neutral gas species) results in an unbounded growth of these parameters within the glow discharge until a glow-to-filamentary transition occurs. Although the instability may be initiated at any step, for the present study, initiation of the IOI chain by heating the surface of the borosilicate glass is thought to occur by increasing the near wall gas temperature, though the possibility of increasing the near wall electron number density due to desorption is not precluded. Additional insight on such processes may be obtained using the modeling approaches of atmospheric filamentary streamers.[10,11]

Regardless of the specific details associated with initiation of the IOI chain, which is identified as the onset of the saturation effect, the data indicate that changing the surface temperature of the dielectric medium of a DBD actuator could stabilize the glow-to-filamentary transition, delaying the saturation effect and increasing the body force, thereby potentially improving the control authority of the actuator.

In summary, the flow field for a DBD actuator prior to and during saturation has been investigated. It was shown that the average fluid velocity decreased upon the inception of filamentary discharge events, which is consistent with reported thrust measurements. Furthermore, it was shown that the saturation effect can be manipulated by changing the surface temperature of the dielectric, resulting in the initiation of the ionization overheating instability chain. These results provide a physics-based explanation for the observations of the many reported parametric studies on the thrust saturation phenomenon.

The first author was supported in part through a DOD SMART scholarship.

[1]U. Kogelschatz, *Plasma Chemistry and Plasma Processing* **23**, 1–46 (2003).
[2]T. C. Corke, C. L. Enloe, and S. P. Wilkinson, Annu. Rev. Fluid Mech. **42**, 505–529 (2010).
[3]E. Moreau, J. Phys. D: Appl. Phys. **40**, 605–636 (2007).
[4]M. Forte, J. Jolibois, J. Pons, E. Moreau, G. Touchard, and M. Cazalens, Exp. Fluids **43**, 917–928 (2007).
[5]F. Thomas, T. Corke, M. Iqbal, A. Kozlov, and D. Schatzman, AIAA J. **47**(9), 2169–2178 (2009).
[6]J. Westerweel, Exp. Fluids **16**, 236–247 (1994).
[7]R. Durscher and S. Roy, Exp. Fluids **53**, 1165–1176 (2012).
[8]A. Fridman and L. A. Kennedy, *Plasma Physics and Engineering* (Taylor & Francis Books, Inc., 2004).
[9]D. Staack, B. Farouk, A. Gutsol, and A. Fridman, J. Appl. Phys. **106**, 013303 (2009).
[10]N. L. Aleksandrovy and E. M. Bazelyanz, J. Phys. D: Appl. Phys. **29**, 740–752 (1996).
[11]C. Li, J. Teunissen, M. Nool, W. Hundsdorfer, and U. Ebert, Plasma Sources Sci. Technol. **21**, 055019 (2012).